# Preconcentration of superbase ionic liquid from aqueous solution by membrane filtration

Filipe H. B. Sosa[1], Pedro J. Carvalho[1], and João A.P. Coutinho[1*].

[1]CICECO – Aveiro Institute of Materials, Department of Chemistry, University of Aveiro, 3810-193 Aveiro (Portugal)

*Corresponding author: João A. P. Coutinho, E-mail address: jcoutinho@ua.pt

## Abstract

Certain organic superbase ionic liquids (ILs) have shown good cellulose dissolution and fiber regeneration performance, allowing to obtain high-quality textile fibers. However, there is a lack regarding the IL recovery from the spinning bath and its purification, which is essential for the economic viability of the process. Aiming to understand methods to separate IL from water for reuse/recycle, the use of pressure-driven membrane processes to recycle ionic liquids from aqueous solution was investigated. The recovery of two superbase ILs, 7-methyl-1,5,7-triazabicyclo[4.4.0]dec-5-enium acetate, [mTBDH][OAc], and 5-methyl-1,5,7-triaza-bicyclo[4.3.0]non-6-enium acetate, [mTBNH][OAc] were studied using different types of membranes (microfiltration, ultrafiltration, nanofiltration and reverse osmosis). Additionally, pressure, IL concentration, temperature and multi-cycles effect were evaluated. Significant retentions (>45%) were obtained for the nanofiltration and reverse osmosis membranes (NF270-NF and BW30LE-RO). The increase in pressure and temperature resulted in an increase in volumetric flux and a decrease in IL retention. On the other hand, IL concentration decreased the volumetric flow and rejection. For the serial filtration tests, a three-fold ionic liquid concentration was achieved, for a maximum concentration of 14 wt% of the ionic liquid. The membrane filtration methodology proved to be an efficient technique for carrying out the preconcentration of the IL from dilute solutions.

**Keywords:** super base Ionic liquid, recovery, nanofiltration, reverse osmosis

# 1. Introduction

The global textile fiber production has almost doubled in the last 20 years, from 58 million tons in 2000 to 109 million tons in 2020. It is estimated that the demand for textile fibers will continue to increase, with a projected production of 134 million tons by 2030, due to population growth and increasing personal consumption.[1] The textile fiber market mainly comprises synthetic fibers (about 60 %), cotton fibers (30 %) and the remaining cellulosic fibers and other natural fibers.[2] Synthetic fibers are mainly produced with non-renewable resources and depend on declining fossil oil resources. On the other hand, wood-based fibers are generally produced from cellulose pulps. However, cellulose must be first dissolved to be used to produce fibers.[3] In industry, the widely used Viscose process (carbon disulfide) produces a large amount of residues (alkaline and acid residues, toxic gases), and in the Lyocell process the explosive NMMO (N-methylmorpholine N-oxide) can cause environmental problems.[4] Therefore, there is a clear need for an alternative sustainable solvent system to produce artificial cellulose fibers. Recently, ionic liquids (ILs) have been proposed as sustainable alternative solvents to produce these fibers.[5,6] Of the several ILs identified as capable of dissolving cellulose, only a small fraction has the characteristics suitable to produce regenerated cellulose fiber (excellent cellulose dissolution and acceptable spinning properties).[7] Recently, 7-methyl-1,5,7-triazabicyclo[4.4.0]dec–5-enium acetate, [mTBDH][OAc], and 5-methyl-1,5,7-triaza-bicyclo[4.3.0]non-6-enium acetate, [mTBNH][OAc] have been identified as promising solvents to produce high-performance fibers.[8,9] Sixta et al.[10] observed in a dissolution study a superior tolerance of [mTBDH][OAc] to solvent-induced changes (water, hydrolysis products and A/B ratio) when compared to [DBNH][OAc]. In this study, good cellulose dissolution was achieved even with a high water content of 10 wt% (58 mol%), demonstrating a pronounced tolerance of [mTBDH][OAc] to the presence of water. Furthermore, [mTBDH][OAc] and [mTBNH][OAc] was more hydrothermally stable than [DBNH][OAc], and the same was found for the stability of the fiber spinning process. In general, these superbases IL have a high potential to be applied in the Ioncell process.

However, after fiber regeneration, the spinning bath contains a variety of contaminants, such as IL, water, and fragments from unregenerated cellulose and some degradation products.[11,12] The recovery of the ILs and their purification is crucial from both an environmental and an economic perspective (Figure S1).

For the separation of water from an ionic liquid, evaporation is widely used due to the low vapor pressure of ILs.[13] However, this process consumes a lot of energy and requires high temperatures, for which some ILs can be degraded. Furthermore, the ILs low volatility can become a problem separating low-volatile solutes (carbohydrates, salts) and heat-sensitive products.[14] Among the various processes used for separation/recovery of ILs, it is possible to highlight the adsorption (activated carbon, resin),[15] extractions (organic solvents, $scCO_2$),[16] crystallization,[17] force field,[18] distillation,[19] and membranes.[20,21]

Membrane separation processes are widely used in the industry as they are cost-effective, simple operation and high efficiency. This methodology is widely used for the treatment of water and sewage. [23] The study with commercial membranes allows the rapid scale-up of the process since these membranes are available on a large scale on the market. In addition, the variety of commercial membranes available enables the selection of the most suitable for each process.

In this sense, the application of membranes (nanofiltration, reverse osmosis, pervaporation) was investigated to purify ILs.[13,22,23]

Along with membrane-based techniques, nanofiltration is one of the most studied techniques to concentrate ILs due to the high purity of the permeates and economical operation. Kröckel and Kragl [20] were one of the first authors to report the application of nanofiltration membranes to separate $[C_4C_1im][BF_4]$ and bromophenol blue in aqueous solution and $[C_1C_1im][CH_3SO_4]$ from lactose. Bromophenol blue and lactose were retained on the membrane while the IL permeated the membrane. Han et al.[24] used nanofiltration to recover ionic liquids from reactions mediated by ionic liquids. The authors report a rejection efficiency of almost 95% for ICYPHOS101 and ECOENG500 ILs in methanol and ethyl acetate solutions using STARMEM$^{TM}$ 120 and 122 nanofiltration membranes. In another study, Hazarika et al.[25] studied the effect of lignocellulose concentration and applied pressure gradients on IL rejection with a commercial nanofiltration membrane (NF270–400, FilmTech). More than 50% of IL was retained by the membrane, with the solvent flow able to be manipulated and increased by increasing the retentate pressure. Comparably, Wang et al.[26] observed that the permeate flux increases with applied pressure when recovering $[C_4C_1im]Cl$ (a recovery rate of up to 96%) with a commercial nanofiltration membrane (NF90-DOW-Filmtec). Abels et al.[27] showed that higher IL concentrations led to a decrease in permeate flux due to low IL permeability and osmotic pressure differences. Haerens et al.[28] reported that the osmotic pressure was the limiting factor on the IL/water separation, for nanofiltration and reverse osmosis membranes. The authors describe only an achievable five-fold ionic liquid concentration for a maximum concentration of 20-25 vol% of the ionic liquid.

Therefore, membrane processes can hardly be used as a single step for separating IL from water, since the osmotic pressure of the target concentration (1-3 wt% of water) would exceed the technical possibilities, so another methodology separator must be used together.

From this perspective, the objective of this work was to pre-concentrate the IL from a synthetic spinning bath solution using membranes. Therefore, the performance of two superbase-based ionic liquid, 7-methyl-1,5,7-triazabicyclo[4.4.0]dec–5-enium acetate, [mTBDH][OAc], and 5-methyl-1,5,7-triaza-bicyclo[4.3.0]non-6-enium acetate, [mTBNH][OAc], that are good candidates to produce high performance cellulose fibres, was studied under different operation conditions. The IL retention, volumetric flux, pressure effect, IL concentration and temperature were evaluated. In addition, the multi-cycles series of nanofiltration and reverse osmosis membranes were evaluated for the purification of IL from an aqueous solution.

# 2. Experimental

## 2.1. Chemical

The superbase-based ionic liquids 7-methyl-1,5,7-triazabicyclo[4.4.0]dec–5-enium acetate, [mTBDH][OAc] (purity >99 %), and 5-methyl-1,5,7-triaza-bicyclo[4.3.0]non-6-enium acetate, [mTBNH][OAc] (purity >97%) were synthesized at the University of Helsinki by stoichiometric mixture (1:1) of acetic acid and the respective superbase (mTBDH or mTBNH) as described elsewhere.[29] In summary, the base was placed in a bottom flask and stirred with a magnetic bar, while acetic acid was added dropwise to the base at 80 °C to avoid crystallization. The purity and structure of ILs synthesis were checked by $^{1}$H-NMR (Figure S2 and S3). The water content of the ILs was determined through the use of a Metrohm 831 Karl-Fischer coulometer, with the analyte Hydranal®-Coulomat AG from Riedel-de Haën. The ultrapure water used to prepare the aqueous solution of ILs was double-distilled, passed through a reverse osmosis system, and further treated with a Milli-Q plus 185 water purification apparatus.

### 2.2. Filtration Procedure

Filtration experiments have been carried out in a stirred cell for flat sheet membranes (Sterlitech HP4750; $V_{max}$: 300 mL, $p_{max}$: 69 bars, active membrane area 14.6 $cm^2$). First, the cell was filled with 75 ml of IL solution, sealed and then pressure (nitrogen, 10 – 50 bars) was applied to permeate the solution. The permeate collected represents a decrease in volume of the original feed solution of 5 to 25%. Supplementary experiments indicate that pseudo steady state operation is attained until about 25% of the original feed volume is permeated (Figure S5). All membranes (MP005-MF, PT-UF, GH-UF, DL-NF, TS80-NF, NF270-NF, BW30LE-NF, UTC-73A-RO) were flushed with pure water before the experiments. The solution to be permeated was constantly stirred at 200 rpm (SCILOGEX SCI550-Pro, hotplate stirrer) to ensure the homogeneity of the system. The permeate was collected in a beaker under an analytical balance (Sartorius LA2000P, $d$ ± 0.001 g) and was quantified over time. The permeate volume was collected for 30 to 60 min, and this value was used to calculate the volumetric flux (Equation 1).

$$F = \frac{V}{t\,A} \qquad (1)$$

where $F$ is the volumetric flux, $V$ is the volume collected in time $t$ and $A$ is the membrane area.

Initial membrane screening was performed with microfiltration, ultrafiltration, nanofiltration and reverse osmose membranes. The detail characteristics of membranes are presented the supplementary material (Tables S1).

Studies with the reverse osmosis membrane (BW30LE-RO) and nanofiltration membrane (NF270-NF) were conducted at five pressures (10, 20, 30, 40, and 50 bars) with a controlled temperature of 298.2 and 313.2 K and different feed concentrations (Table 1). The BW30LE-RO and NF270-NF membranes were chosen because they were designed to operate at lower pressures, with similar fluxes.[28]

The IL concentration in the permeate and retentate solution was determined at 303.2 K using an Anton Paar Abbemat 5010 refractometer, with an uncertainty of $2 \cdot 10^{-5}$ nD. A calibration curve was previously performed using standards with different compositions (uncertainty of $10^{-4}$ g).

IL rejection was determined by Equation 2:

$$R_{IL} = \left(1 - \frac{c_{ILp}}{c_{ILf}}\right).100\% \qquad (2)$$

where $R_{IL}$ is the rejection of IL, $c_{ILp}$ is the concentration of IL in the permeate solution and $c_{ILf}$ is the concentration of IL in the feed solution.

**Table 1.** List of membranes, feed streams and tested conditions.

| Membrane | Conditions (agitation 200 rpm) | | |
|---|---|---|---|
| | IL Concentration | Pressure | Temperature |
| MP005-MF, PT-UF, GH-UF, DL-NF, TS80-NF, NF270-NF, BW30LE-NF, UTC-73A-RO | 1 wt% [mTBDH][OAc] | 10 bars | 298.2 K |
| | 1 wt% [mTBNH][OAc] | 10 bars | 298.2 K |
| BW30LE-RO, NF270-NF | 1 wt% [mTBDH][OAc] | 10-50 bar | 298.2 K |
| | 1 wt% [mTBNH][OAc] | 10-50 bar | 298.2 K |
| | 1, 5, 10, 15, 20 wt% [mTBDH][OAc] | 40 bars | 298.2 K |
| | 1, 5, 10, 15, 20 wt% [mTBNH][OAc] | 40 bars | 298.2 K |
| | 1, 15 wt% [mTBDH][OAc] | 40 bars | 298.2/313.2K |
| | 1, 15 wt% [mTBNH][OAc] | 40 bars | 298.2/313.2K |

## 2.3. Membrane Cleaning

The process of membrane fouling results in the loss of performance (in terms of flow) of a membrane due to the presence of suspended or dissolved substances in the membrane's pores.[30] In order to avoid such process, a chemical cleaning of the membrane was carried out between each experiment. In this way, guaranteeing the same membrane performance throughout the tests was possible.

The cleaning procedure consisted of firstly permeating the membrane with an aqueous solution of sodium hydroxide (0.1 %) for 45 minutes (at 313.2 K and 15 bars), then permeating the membrane with an aqueous solution of sulfuric acid (0.2 %) for 45 minutes (at 313.2 K and 15 bars) and finally check the permeation flux of the membrane with ultra-pure water at 298.2 K and 10 bars (Figure S6). If the flow is lower than that obtained in the previous test, the cleaning process was repeated. After use, all membranes were rinsed with water and stored in an aqueous solution of 1% sodium metabisulfite to prevent bacterial growth.

# 3. Results

Membrane filtration is a process of removing/separating substances by forcing the solution to permeate through a porous medium. Different factors can affect membrane efficiency. The main membrane characteristics controlling the filtration efficiency are the membrane properties, pore size, hydrophobicity, and pore size distribution and material. On the other hand, the solution properties, solution concentration, particle size and nature of compounds are also essential.[28] Considering this, a study was conducted with various types of membranes with different pore sizes to evaluate the recovery of superbase IL from an aqueous solution.

## 3.1. Membrane screening

The volumetric flux and rejection of substances can be affected by several filtration factors, such as transmembrane pressure, temperature, osmotic pressure, substance concentration and other membrane characteristics (porosity, density). At first, eight membranes were selected (MP005-MF, PT-UF, GH-UF, DL-NF, TS80-NF, NF270-NF, BW30LE-NF, UTC-73A-RO) with different porosities and densities. The permeation flux and the IL rejection of diluted IL aqueous solutions (1 wt%) were determined by applying a transmembrane pressure of 10 bars, at 298.2 K, on these membranes. The stability and integrity of the IL after filtration were investigated by NMR and FTIR. The band assignments were performed according to IR spectrum table by frequency range reported in the literature.[31] Characteristic IL absorption bands related to C-N stretching (1342 - 1266 $cm^{-1}$), O-H bending (1440 - 1395 $cm^{-1}$), C=N stretching (1690 - 1640 $cm^{-1}$) and O-H stretching (3200-2700 $cm^{-1}$) were observed in all spectra, suggesting no changes in the IL structure after membrane treatments

(Figure S4). The $^{1}$H-NMR and $^{13}$C-NMR spectra with chemical shift of ILs before and after permeation were presented in Figure S2 and Figure S3. The chemical shift difference of the peak's signals of both IL before and after permeation were insignificant. For example, the chemical shift of hydrogens in the acetate of [mTBDH][OAc] presented a value of 1.60 ppm for both samples before and after permeation. Therefore, the IL remains intact without modification in the chemical structure or molar ratio of IL cation/anion, remaining stable and intact after permeation.

Figure 1 shows the experimental volumetric flux and IL rejection of aqueous solutions containing 1 wt% of IL. It can be seen that the volumetric fluxes, at 10 bars, followed the order of MP005-MF > PT-UF > TS80-NF > DL-NF > GH-UF > NF270-NF > BW30LE-NF > UTC-73A-RO. The correlation between membrane porosity and volumetric flux is presented in Figure S7. The maximum volumetric flux was observed for the solution of 1 wt% of [mTBNH][OAc] with the membrane MP005-MF (2494.8 L $m^{-2}$ $h^{-1}$), and the minimum for the solution of 1 wt% of [mTBDH][OAc] with UTC-73A-RO membrane (5.8 L $m^{-2}$ $h^{-1}$). The differences in membrane porosity may explain this behavior.

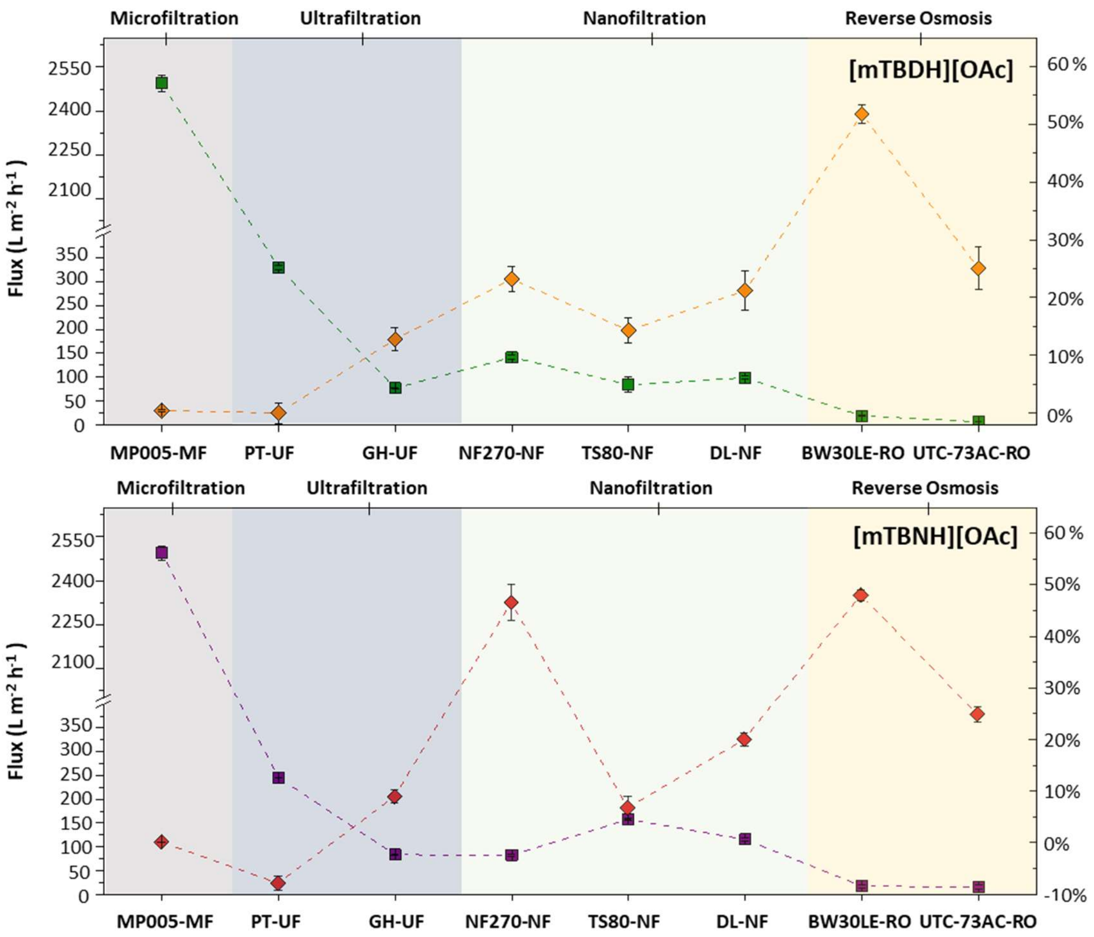


**Figure 1.** Effect of membrane on the volumetric flux ((■) [mTBDH][OAc] and (■) [mTBNH][OAc]) and IL rejection ((♦) [mTBDH][OAc] and (♦) [mTBNH][OAc]). Conditions: solution of 1 wt% of [mTBDH][OAc] or [mTBNH][OAc], 10 bars, 200 rpm at 298.2 K. Dashed lines are visual guides

Microfiltration membranes (MF) have pores of up to 0.1µm, which do not offer any resistance to the passage of IL molecules. Furthermore, they are commonly used at pressures below 1 bar, so at pressures of 10 bar, flows tend to be higher with almost no IL rejection.[32] Ultrafiltration membranes (UF) have a smaller pore size, in the nanometer range (2–100 nm), in addition to higher porosity, which leads to a certain resistance to the passage of the IL.[33] Nanofiltration (NF) membranes, on the other hand, have a pore size of less than 1 nm, and are able to retain part of the IL.[34] In the case of the NF270-NF membrane, rejection values of 46.5% were obtained. Unlike others, reverse Osmosis (RO) membranes are not porous but dense, this causes the IL to diffuse through the membrane.[35] Due to its larger molecular volume, IL tends to have a slower diffusion through the membrane when compared to water molecules, and therefore the rejection tends to be higher for this type of membrane (>45%). In the case of [mTBNH][OAc], the IL rejection order is: BW30LE-NF> NF270-NF> UTC-73A-RO > DL-NF > TS80-NF ≈ GH-UF > MP005-MF > PT-UF.

However, the size of the molecules is not the only factor that affects the separation efficiency, the interactions of the molecules with the membrane as well as the charge of the ions or molecules, influence the retention.[36] Since the ion charge exclusion depends on the membrane charges, the ionic force and the ion valence.[37] Avram et al.[21] observed that the size-based separation alone was ineffective in separating IL and low molecular weight sugars (glucose). The authors indicate that controlling the thickness and structure of the layer was essential to maximize the rejection of sugar. In addition, the volumetric flux is reduced, and RO generally requires high transmembrane pressures to operate in industrial processes.

Except for the PT-UF membrane, part of the IL can be retained in all other membranes, whereas the water permeates. In the case of PT-UF, most water can be retained whereas the IL permeates through the membrane. In this case, the limiting factor of the separation was the affinity between the IL molecule and the membrane surface and not the porosity/density of the membrane.

Remarkably, the NF270-NF membrane showed IL rejection rates comparable to reverse osmosis membranes (BW30LE-RO and UTC-73AC-RO). This implies that for some situations, it is possible to obtain the same IL rejection but with a much higher volumetric flow (4.5 times), allowing for a more efficient filtration process from an operational point of view.

Based on the membrane screening results, the NF270-NF (IL rejection > 23%) and BW30LE-RO (IL rejection > 48%) membranes were selected and the effect of pressure, feed IL concentration and the effect of temperature were further evaluated.

## 3.2. Pressure Effect

In order to evaluate the pressure effect during the filtration of superbase ILs with NF270-NF and BW30LE-RO membranes, a series of filtrations, presented in Figure 2, were performed at different pressures (10, 20, 30, 40, 50 bars). During the filtration of an IL solution ([mTBDH][OAc] and [mTBNH][OAc])) with the NF270 membrane, the IL rejection increases with increasing pressure, reaching a maximum value followed by a decrease. This behavior differs from most trends reported in the literature for nanofiltrations of binary mixtures. At first, an increase in retention with increasing pressure is observed, followed by a smaller increase or stabilization at higher pressures.[38–40] For example, Wang et al.[26] evaluated the filtration behavior of ILs ([AMIM]Cl, [BMIM]Cl and [BMIM][$BF_4$]) in an aqueous solution by NF270-NF. The authors observed that the permeate flux and IL rejection increased with the pressure applied at a constant IL concentration.

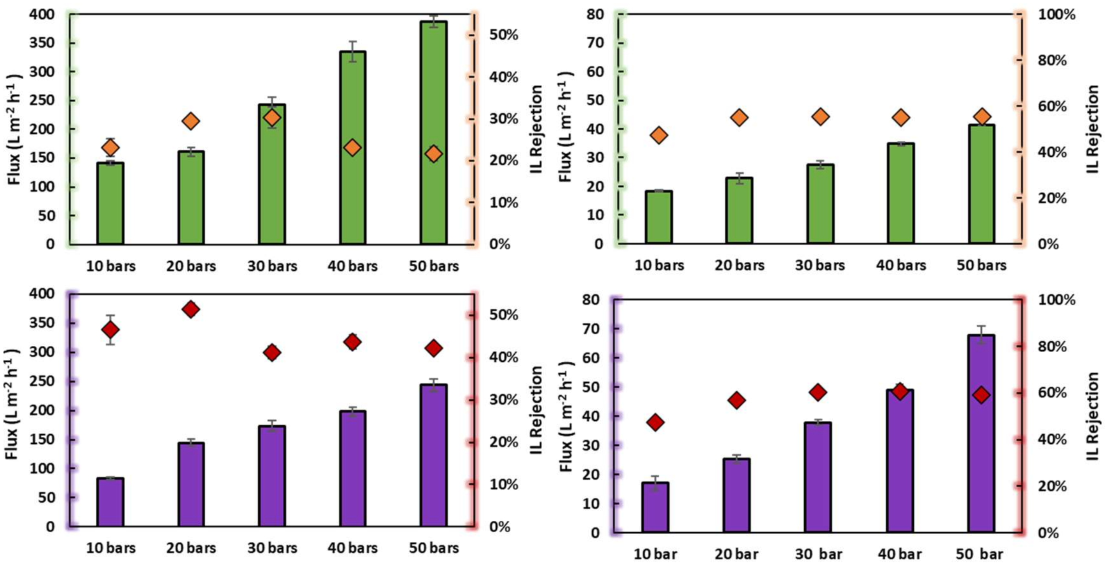


**Figure 2.** Effect of pressure on the performance of NF270-NF (left) and BE30LE-RO (right): volumetric flux (■) [mTBDH][OAc] and (■) [mTBNH][OAc] and IL rejection (♦) [mTBDH][OAc] (♦) [mTBNH][OAc]. Conditions: 1 wt% [mTBDH][OAc] or [mTBNH][OAc] , 10, 20, 30, 40, 50 bars, 200 rpm at 298.2 K.

However, a maximum retention peak with increasing pressure for some systems has been reported.[41,42] The authors attribute this behavior to the effect of an increase in the polarization layer with pressure when the cross flow velocity is low.[42] Nevertheless, in the results obtained in this study, the volumetric flux of the permeate tends to increase linearly with pressure. Xu and Lebrun [43] consider this linearity due to the absence of concentration polarization. Therefore, the decrease in rejection after a given pressure cannot be justified regarding the concentration polarization phenomenon.

Since NF270-NF is a porous membrane, the IL would be expected to enter the membrane pore (whose cut-off diameter is 200-400 Da) and remain partially retained due to membrane surface forces.[44] As pressure increases, surface forces remain constant while drag forces increase due to increased pore flow. At low pressures, surface forces tend to be stronger than drag forces. Therefore, the IL flow remains low, while the water flow increases with pressure, resulting in an increased IL rejection. Above a certain pressure, drag forces become higher than surface forces, and, consequently, the solute transfer increases and the retention decreases.[45]

Abels et al.[27] evaluated the IL rejection of IL/water mixture with IL mass fraction ranging from 0 to 80 wt% by two commercially available polyamide and one polyimide membranes (Desal DL, Desal DK and Starmem 240). At low IL concentrations, the effect of pressure played a significant role in the IL rejection. However, at high IL concentrations, the pressure effect is less pronounced.

For the BW30LE-RO membrane, increased retention is observed with increasing pressure, followed by stabilization at higher pressures. Concerning volumetric flow, the increase in pressure results in a linear increase in volumetric flow. This plateau can be beneficial in the industrial operation of reverse osmosis membranes since at higher pressures, the IL rejection rates are the same as at lower pressures. Still, the permeate fluxes are higher, making the process more efficient.[46]

### 3.3. IL feed concentration Effect

In general, membrane permeation is more difficult for large molecules than for smaller molecules, so the transmembrane pressure tends to increase with the size of the molecule. However, the composition of the medium, more specifically the concentration, also has an effect on membrane performance.[47]

The relation between membrane performance (volume flow and IL rejection) and ionic liquid concentration in the feed solution is shown in Figure 3.

With the increased IL concentration in the feed solution, a reduction of the volumetric flux is observed. For example, for the BW30LE-RO membrane no volumetric flux was observed for the concentration of 20 wt% of IL.

Regarding IL rejection, the results show that the increase in concentration decreases IL retention. Wang et al.[26] reported the same behavior with the filtration of aqueous solutions of [BMIM][Cl] and [AMIM][Cl] by nanofiltration membranes (NF90 and NF270). This behavior is characteristic of this membrane type and is generally interpreted by the shielding phenomenon.[39,48] This effect is mainly attributed to the cation shielding of the effective charge of the membrane. This characteristic can be explained by the electrical repulsion becoming less efficient at higher concentrations since there is a tendency to form an IL film on the membrane that gradually neutralizes the charges on its surface. Consequently, the repulsive forces decreased, so the rejection rate was slightly reduces.[49]

This effect tends to be weak at low concentrations, so high retention is expected. However, a low IL retention rate was observed for the 1 wt% solution. This behavior is related to the high volumetric flux, in which the drag forces overcome the surface forces, decreasing IL rejection.[45] When the concentration is higher, this effect tends to be more prominent, and the membrane potential weakens. Abels et al.[27] observed at higher ionic liquid concentrations that no separation of IL from the mixture was achieved using polyamide membranes (Desal DL and Desal DK). Furthermore, as the repulsion between the membrane and the ions decreases, they tend to cross the membrane more quickly, thus dragging the other ions and retention is thus decreased.[45]

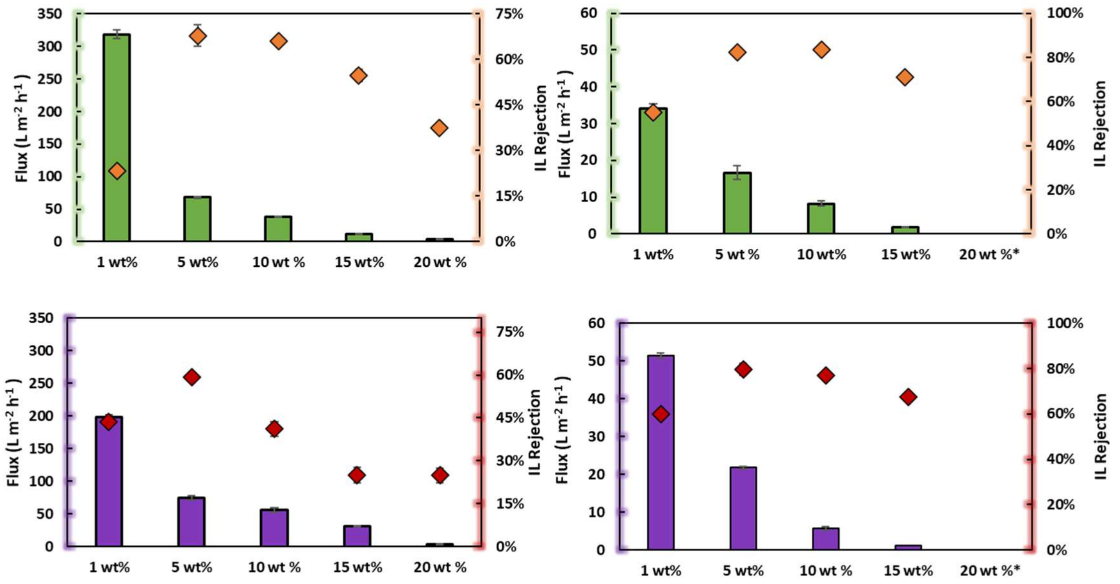


*No flux was observed under these conditions

**Figure 3.** Effect of feed IL concentration on the performance of NF270-NF (left) and BW30LE-RO (right): volumetric flux (■) [mTBDH][OAc] and (■) [mTBNH][OAc], and IL rejection (♦) [mTBDH][OAc] (♦) [mTBNH][OAc]. Conditions: 1, 5, 10, 15, 20 wt% [mTBDH][OAc] or [mTBNH][OAc] 200 rpm at 40 bars and 298.2 K.

Therefore, the concentration of the IL solution plays a crucial role in the case of membrane fouling, which alters the performance characteristics, resulting not only in a significant decrease in flux or permeability but also in reduced IL rejection.[48]

### 3.4. Temperature effect

The nanofiltration and reverse osmosis membranes are designed to operate at room temperature. However, their use at temperatures above ambient may provide better performance depending on the conditions and feed solution.[50]

The effect of temperature (studied at 298.2 and 313.2 K) on membrane performance is shown in Figure 4. It is shown that while the volumetric fluxes of the membrane improve, the rejection rate decreases with increasing temperature. The temperature increase in solute transport is mainly related to the cumulative effect of reducing solvent viscosity and increasing ion diffusivity. Therefore, this effect is more pronounced for more concentrated solutions (15 wt%).[49] Nilsson et al.[51] did not observe significant changes in the isoelectric point of the NFT-50 membrane (Alpha Laval) with temperature variation, concluding that the membrane charge properties are not significantly affected by the temperature increase. However, other parameters such as solvent viscosity, solute diffusivity, and structural parameters tend to be affected with increasing temperature. The effect of modifying these parameters with temperature has a direct impact on the passage of ions.[52] However, Abel et al.[27] observed that the increase in temperature had a minor effect on the permeability of IL, even though the viscosity decreased. In general, it is not enough to consider only the change in solvent viscosity or solute diffusivity to explain the increase in volumetric flux and the reduction in IL rejection. A study of the structural parameters of the membrane, which were not studied in this work, is necessary.[52]

Therefore, for the conditions tested, increasing temperature results in an improvement in volumetric membrane fluxes and a slight reduction in IL retention. The use of temperature can be a solution for high concentrated or viscous solutions.

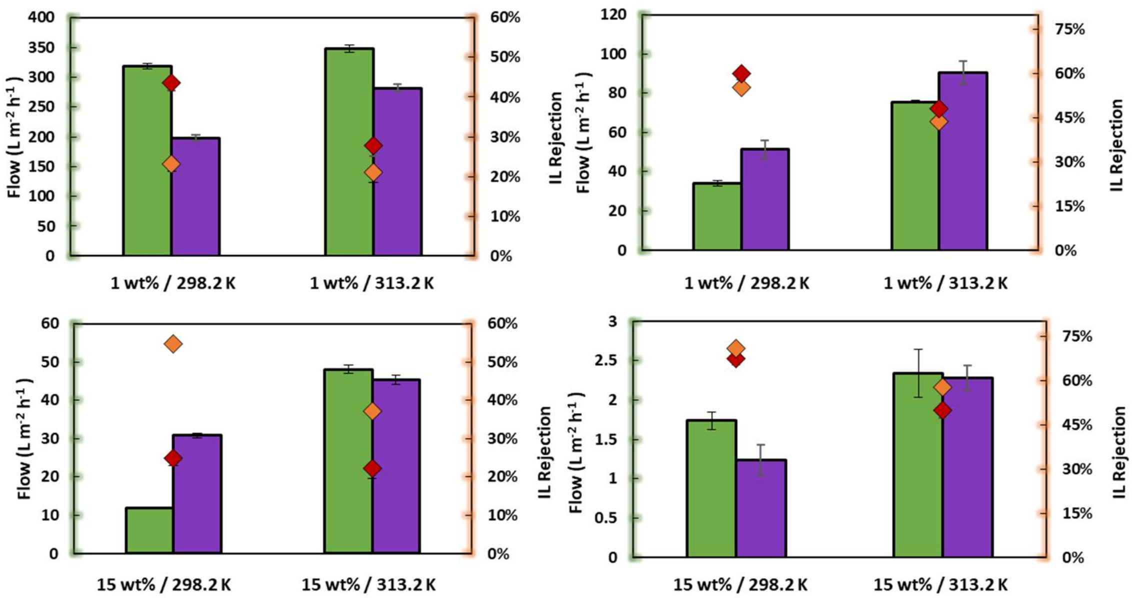


**Figure 4.** Temperature effect on the performance of NF270-NF (left) and BW30LE-RO (right): volumetric flux (■) [mTBDH][OAc] and (■) [mTBNH][OAc], and IL rejection (♦) [mTBDH][OAc] (♦) [mTBNH][OAc]. Conditions: 1 and 15 wt% [mTBDH][OAc] or [mTBNH][OAc] 200 rpm at 40 bars and 298.2 or 313.2 K.

## 3.5. Multi-cycle filtration

Multi-cycle membrane filtration experiments were used to simulate the continuous operation membrane that is foreseeable at an industrial scale. The cycles using the nanofiltration and the reverse osmose filtration membranes were performed. Each nanofiltration cycle included 15 minutes of filtration followed by a chemical and water cleaning process. The reverse osmose filtration cycles comprised 90 minutes of filtration followed by a chemical and water cleaning cycle. As shown before, a long time was required due to the low volumetric flux obtained with the reverse osmosis membrane.

At each cycle, an increase in the concentration of the retentate was observed. As previously discussed, this behavior directly impacts the volumetric flux and retention of the IL, due to the increase in the concentration of the solution

(Figure 5). For NF270-NF membrane, permeate concentration increases with each cycle, this means that the IL retention efficiency decreases with the increase of solution concentration.

During the cycles, it was possible to concentrate the initial solution (5 wt%) of IL about 1.5 and 2.9 times for NF270-NR and BW30LE-RO, respectively. In the nanofiltration, cycle 4 is the longest cycle (approx 50 min), and in this cycle, it was possible to concentrate an initial solution from 7.7 wt% to 12.3 wt % of [mTBNH][OAc]. This longer cycle allowed us to observe that there is a tendency to stabilize the IL retention as well as the concentration in the permeate with increasing filtration time. Another critical point to highlight is that the concentration of IL in the permeate of NF270-NF is higher than the concentration of IL in the BW30LE-RO permeate.

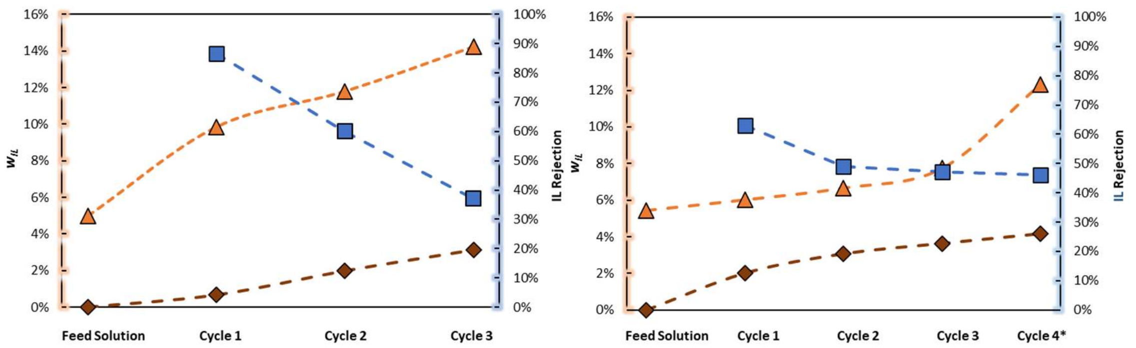


**Figure 5.** Multi-cycle membrane filtration experiments of NF270-NF (left) and BW30LE-RO (right): [mTBNH][OAc] concentration in the retentate (▲) [mTBNH][OAc] concentration in the permeate (♦) [mTBNH][OAc], and IL rejection (■) of each cycle. Conditions: 5 wt% [mTBNH][OAc] 200 rpm at 40 bars and 298.2 K. Dashed lines are visual guides.

With the parameters of IL rejection, permeate, and retentate concentration, as well as the volumetric fluxes, it was possible to propose filtration scenarios combining nanofiltration membrane and reverse osmosis (Figure 6). Calculations were performed for filtration of a solution containing 5 wt% of [mTBNH][OAc] and flow of 100 L $h^{-1}$ in a series of NF270-NF and BW30LE-RO membranes. In scenarios A and B, the IL permeates concentration increases, and the permeate flux decreases every new cycle. This behavior is a result of the increase in the IL feed concentration in each new cycle, which as verified, affects the IL rejection. At the end of the fifth cycle in scenario A, it was possible to concentrate the IL in a solution containing 14 wt% (R5). The permeate streams were combined (mixture containing ≈ 3.8 wt% IL) and filtered through two BW30LE-RO membranes. From the BW30LE membranes, two streams resulted, the permeate stream (P7) with a diluted IL solution (0.2 wt% IL) and the retentate stream (R6) with a concentration of 5 wt% IL, the same concentration as the feed. Therefore, the retentate stream can be fed back into the system, as shown in the diagram (Figure 6).

In scenario B, the permeate stream from the second nanofiltration membrane (P2) was filtered by NF270-NF membrane. The retentate from that filtration (R5) was mixed with the permeate stream from the first membrane (P1) and fed into a BW30LE-RO. Then, the P5 stream was combined with the permeate of the third NF270-NF (P3) and fed into a reverse osmosis membrane. Thus, it was possible to obtain a concentrated IL stream (R3 ≈ 12.8 wt% IL). The stream R7 (≈ 8.6 wt% IL) can be fed back into the third NF270-NF membrane with stream R2, the P4 stream can be combined with P2 stream and be fed into the NF270-NF, and streams R6 and P4 (≈ 3.5 wt% IL) mixed and fed through a reverse osmosis membrane.

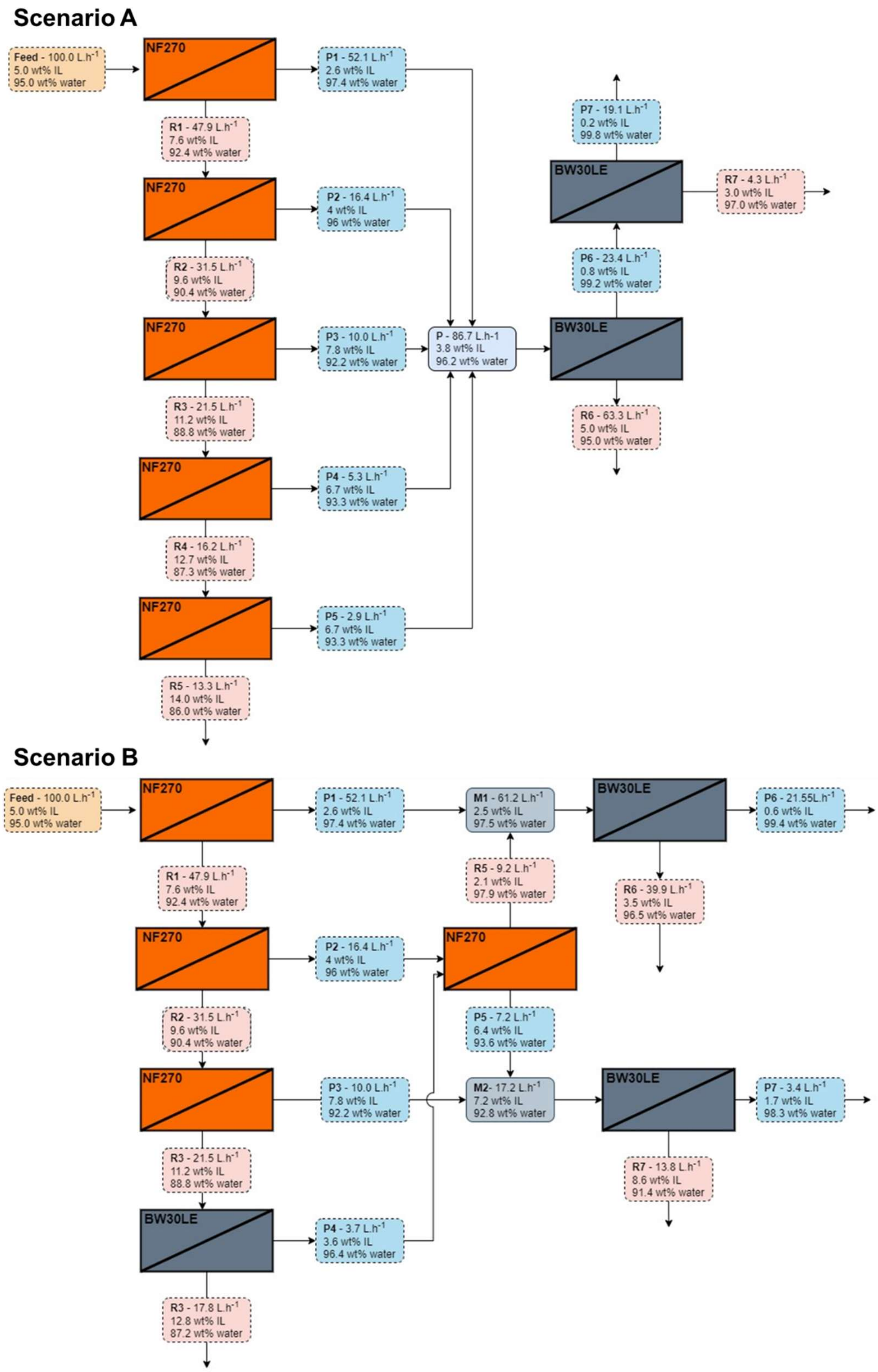


**Figure 6**. Flowchart of the proposed filtration Scenario A and Scenario B combining nanofiltration and reverse osmosis membrane. Conditions: 5 wt% [mTBNH][OAc] 200 rpm at 40 bars and 298.2 K.

In general, under the optimal experimental parameters, the aqueous solution of IL at 5 wt% can be concentrated to approximately 14 wt%. The configuration of the membranes in the proposed scenario allowed to obtain a water stream practically without IL (≈ 0.2 wt% IL), an advantage for the process since the main purpose is to remove water from the IL solution.

Furthermore, the streams with low IL concentration can be fed into other membranes, for example, reverse osmosis membranes which would allow a significant reduction in IL loss, resulting in a stream with pure water and a concentrated stream in IL. Combining nanofiltration and reverse osmosis membranes is essential to avoid IL loss during filtration and ensure minimal flow to feed other membranes. Since the results showed that the nanofiltration membrane (NF270-NF) has IL rejection rates similar to reverse osmosis (BW30LE-RO) for dilute solutions, but with higher fluxes. These results provide the fundamental data necessary for applying nanofiltration and reverse osmosis technology to preconcentrate IL from spinning bath.

It is important to emphasize that the concentration reached at the end of the filtration (≈ 14 wt%) is far from the concentration required (≈ 80 wt%) to reuse IL with the same cellulose dissolution capacity. Sixta et al. [9] used a set of heat treatment operations (centrifugal evaporator) to concentrate the spinning bath. With this approach, obtaining an IL solution with low residual water content (2.2 - 3.1 wt%) was possible. However, the authors reported that the energy demand for the recovery of dilute IL solutions (0.1 -1.5 wt% IL) is tremendously high. Therefore, it reinforces this study approach to utilize membrane treatment to pre-concentrate the spinning bath solution.

In order to compare the ILs recovery technique by membrane filtration and distillation, energy expenses were preliminarily calculated to support the proposed conclusions. For this, the software Aspen Plus V12.1 was used. The model design was based on a COSMO-SAC method. Distillation was simulated with a Radfrac distillation column with a reboiler only (Figure S8). The feed stream was a solution containing 5 wt% of [mTBNH][OAc] and a flow of 100 L $h^{-1}$. It was defined as a specification that the IL current should have a concentration of 15 wt% IL, the same value obtained for the membrane scenarios. To determine the energy expenses of the membranes, a hydraulic turbine was used, and the pressure set was 40 bars.

For distillation, an energy expense of 4790.6 $W/kg_{Feed}$ was obtained, while for filtration, the expenditure was only 2.6 $W/kg_{Feed}$. The energy expenditure required for the membranes is lower when compared to distillation since it is not necessary to vaporize the water, which in this scenario comprises up about 95% of the solution. These results emphasize the idea that membrane filtration technology should be considered in the preconcentration stage of the IL spinning bath since there is a large amount of water to be removed at this stage.

On the other hand, distillation can be applied to a subsequent concentration step when the solution is already more concentrated, and the IL rejections by the membranes tend to decrease.

## 4. Conclusions

In this work, the filtration behavior of aqueous solutions of two superbase ionic liquids, [mTBDH][OAc] and [mTBNH][OAc] using microfiltration, ultrafiltration, nanofiltration and reverse osmosis membranes were studied.

Nanofiltration (NF270-NF) and reverse osmosis (BW30LE-RO) membranes showed the highest capacity for retention/separation of IL from the diluted aqueous solution (>45%). For these membranes, the volumetric flux of permeate increased linearly with increasing pressure applied at constant IL concentration and decreased with increasing IL concentration in the feed solution at constant pressure.

Compared to the nanofiltration membrane (NF270-NF), the reverse osmosis membrane (BW30LE-RO) showed the highest retention due to its smaller pore size. Regarding IL rejection, the results show that the increase in concentration decreases IL retention. The use of higher temperatures (313.2 K) resulted in an increase in the volumetric flow of the membrane and consequently a reduction in the IL rejection rate. Using the filtration membrane in a series of cycles allowed to concentrate the initial solution of 5 wt% to 14 wt% of IL.

From these results, it is possible to remark that membrane filtration can hardly be used as a single step for separating IL from water since the maximum IL concentration obtained (14 wt%) is lower than the desired (80 wt%) for IL reuse. Therefore, complete separation of IL and water can be achieved by combining different separation methods, such as distillation and membrane separation. Thus, it is possible to reach the desired IL concentration using distillation and reduce the energy demand for diluted solutions with membrane filtration.

## Supporting Information

IL characterization ($^1$H-NMR); Specification of membranes; Water permeation flux (NF270-NF and BW30LE-RO); Retentate and Permeated characterization ($^1$H-NMR)

## Notes

The authors declare that they have no known competing financial interests or personal relationships that could have appeared to influence the work reported in this paper

## CRediT authorship contribution statement

**Filipe H.B. Sosa:** Conceptualization, Methodology, Investigation, Data curation, Writing–original draft, Visualization. **Pedro J. Carvalho:** Conceptualization, Methodology, Writing –review & editing. **João A.P. Coutinho**: Conceptualization, Data curation, Writing–review & editing, Supervision, Funding acquisition

## Acknowledgments

This work was developed within the scope of the GRETE project funded from the Bio-Based Industries Joint Undertaking under the European Union's Horizon 2020 research and innovation programme under grant agreement No 837527 – GRETE – H2020-BBI-JTI-2018. Additionally, this work was developed within the scope of the project CICECO Aveiro Institute of Materials, UIDB/50011/2020, UIDP/50011/2020 & LA/P/0006/2020, financed by national funds through the FCT/MEC (PIDDAC).

## References

(1) Textile Exchange. Preferred Fiber & Materials Market Report 2021. **2021**, 1–118.

(2) Bureau, I. *CIRFS: European Man-Made Fibers Association*. 2014.

(3) Wang, S.; Lu, A.; Zhang, L. Recent Advances in Regenerated Cellulose Materials. *Prog. Polym. Sci.* **2016**, *53*, 169–206.

(4) Sayyed, A. J.; Deshmukh, N. A.; Pinjari, D. V. A Critical Review of Manufacturing Processes Used in Regenerated Cellulosic Fibres: Viscose,

Cellulose Acetate, Cuprammonium, LiCl/DMAc, Ionic Liquids, and NMMO Based Lyocell. *Cellulose* **2019**, *26* (5), 2913–2940.

(5) Mäki-Arvela, P.; Anugwom, I.; Virtanen, P.; Sjöholm, R.; Mikkola, J. P. Dissolution of Lignocellulosic Materials and Its Constituents Using Ionic Liquids-A Review. *Ind. Crops Prod.* **2010**, *32* (3), 175–201.

(6) King, A. W. T.; Asikkala, J.; Mutikainen, I.; Järvi, P.; Kilpeläinen, I. Distillable Acid-Base Conjugate Ionic Liquids for Cellulose Dissolution and Processing. *Angew. Chemie - Int. Ed.* **2011**, *50* (28), 6301–6305.

(7) Xu, A.; Wang, F. Carboxylate Ionic Liquid Solvent Systems from 2006 to 2020: Thermal Properties and Application in Cellulose Processing. *Green Chem.* **2020**, *22* (22), 7622–7664.

(8) Elsayed, S.; Hummel, M.; Sawada, D.; Guizani, C.; Rissanen, M.; Sixta, H. Superbase-Based Protic Ionic Liquids for Cellulose Filament Spinning. *Cellulose* **2021**, *28* (1), 533–547.

(9) Elsayed, S.; Hellsten, S.; Guizani, C.; Witos, J.; Rissanen, M.; Rantamäki, A. H.; Varis, P.; Wiedmer, S. K.; Sixta, H. Recycling of Superbase-Based Ionic Liquid Solvents for the Production of Textile-Grade Regenerated Cellulose Fibers in the Lyocell Process. *ACS Sustain. Chem. Eng.* **2020**, *8* (37), 14217–14227.

(10) Elsayed, S.; Viard, B.; Guizani, C.; Hellsten, S.; Witos, J.; Sixta, H. Limitations of Cellulose Dissolution and Fiber Spinning in the Lyocell Process Using [MTBDH][OAc] and [DBNH][OAc] Solvents. *Ind. Eng. Chem. Res.* **2020**, *59* (45), 20211–20220.

(11) Lopes, J. M.; Bermejo, M. D.; Martín, Á.; Cocero, M. J. Ionic Liquid as Reaction Media for the Production of Cellulose-Derived Polymers from Cellulosic Biomass. *ChemEngineering* **2017**, *1* (2), 1–28.

(12) Yang, J.; Lu, X.; Yao, X.; Li, Y.; Yang, Y.; Zhou, Q.; Zhang, S. Inhibiting Degradation of Cellulose Dissolved in Ionic Liquids: Via Amino Acids. *Green Chem.* **2019**, *21* (10), 2777–2787.

(13) Sklavounos, E.; Helminen, J. K. J.; Kyllönen, L.; Kilpeläinen, I.; King, A. W. T. Ionic Liquids: Recycling. In *Encyclopedia of Inorganic and Bioinorganic Chemistry*; John Wiley & Sons, Ltd: Chichester, UK, 2016; pp 1–16.

(14) King, A. W. T.; Parviainen, A.; Karhunen, P.; Matikainen, J.; Hauru, L. K. J.; Sixta, H.; Kilpeläinen, I. Relative and Inherent Reactivities of Imidazolium-Based Ionic Liquids: The Implications for Lignocellulose Processing Applications. *RSC Adv.* **2012**, *2* (21), 8020–8026.

(15) Anthony, J. L.; Maginn, E. J.; Brennecke, J. F. Solution Thermodynamics of Imidazolium-Based Ionic Liquids and Water. *J. Phys. Chem. B* **2001**, *105* (44), 10942–10949.

(16) Honglu, X.; Tiejun, S. Wood Liquefaction by Ionic Liquids. *Holzforschung* **2006**, *60* (5), 509–512.

(17) Liu, Y.; Meyer, A. S.; Nie, Y.; Zhang, S.; Thomsen, K. Low Energy Recycling of Ionic Liquids: Via Freeze Crystallization during Cellulose

Spinning. *Green Chem.* **2018**, *20* (2), 493–501.

(18) Birdwell, J. F.; McFarlane, J.; Hunt, R. D.; Luo, H.; DePaoli, D. W.; Schuh, D. L.; Dai, S. Separation of Ionic Liquid Dispersions in Centrifugal Solvent Extraction Contactors. *Sep. Sci. Technol.* **2006**, *41* (10), 2205–2223.

(19) Elsayed, S.; Hellsten, S.; Guizani, C.; Witos, J.; Rissanen, M.; Rantamäki, A. H.; Varis, P.; Wiedmer, S. K.; Sixta, H. Recycling of Superbase-Based Ionic Liquid Solvents for the Production of Textile-Grade Regenerated Cellulose Fibers in the Lyocell Process. *ACS Sustain. Chem. Eng.* **2020**, *8* (37), 14217–14227.

(20) Kröckel, J.; Kragl, U. Nanofiltration for the Separation of Nonvolatile Products from Solutions Containing Ionic Liquids. *Chem. Eng. Technol.* **2003**, *26* (11), 1166–1168.

(21) Avram, A. M.; Ahmadiannamini, P.; Qian, X.; Wickramasinghe, S. R. Nanofiltration Membranes for Ionic Liquid Recovery. *Sep. Sci. Technol.* **2017**, *52* (13), 2098–2107.

(22) Zhou, J.; Sui, H.; Jia, Z.; Yang, Z.; He, L.; Li, X. Recovery and Purification of Ionic Liquids from Solutions: A Review. *RSC Adv.* **2018**, *8* (57), 32832–32864.

(23) Sirkar, K. K. Membrane separation technologies: current developments. *Chem. Eng. Commun.* **1997**, *157* (1), 145–184.

(24) Han, S.; Wong, H. T.; Livingston, A. G. Application of Organic Solvent Nanofiltration to Separation of Ionic Liquids and Products from Ionic Liquid Mediated Reactions. *Chem. Eng. Res. Des.* **2005**, *83* (3 A), 309–316.

(25) Hazarika, S.; Dutta, N. N.; Rao, P. G. Dissolution of Lignocellulose in Ionic Liquids and Its Recovery by Nanofiltration Membrane. *Sep. Purif. Technol.* **2012**, *97*, 123–129.

(26) Wang, J.; Luo, J.; Zhang, X.; Wan, Y. Concentration of Ionic Liquids by Nanofiltration for Recycling: Filtration Behavior and Modeling. *Sep. Purif. Technol.* **2016**, *165*, 18–26.

(27) Abels, C.; Redepenning, C.; Moll, A.; Melin, T.; Wessling, M. Simple Purification of Ionic Liquid Solvents by Nanofiltration in Biorefining of Lignocellulosic Substrates. *J. Memb. Sci.* **2012**, *405–406*, 1–10.

(28) Haerens, K.; Van Deuren, S.; Matthijs, E.; Van der Bruggen, B. Challenges for Recycling Ionic Liquids by Using Pressure Driven Membrane Processes. *Green Chem.* **2010**, *12* (12), 2182–2188.

(29) Martins, M. A. R.; Sosa, F. H. B.; Kilpeläinen, I.; Coutinho, J. A. P. Physico-Chemical Characterization of Aqueous Solutions of Superbase Ionic Liquids with Cellulose Dissolution Capability. *Fluid Phase Equilib.* **2022**, 113414.

(30) Al-Amoudi, A.; Williams, P.; Mandale, S.; Lovitt, R. W. Cleaning Results of New and Fouled Nanofiltration Membrane Characterized by Zeta Potential and Permeability. *Sep. Purif. Technol.* **2007**, *54* (2), 234–240.

(31) *IR Spectrum table by frequency range*. https://www.sigmaaldrich.com/PT/en/technical-documents/technical-article/analytical-chemistry/photometry-and-reflectometry/ir-spectrum-table.

(32) Van der Bruggen, B. *Microfiltration, Ultrafiltration, Nanofiltration, Reverse Osmosis, and Forward Osmosis*; Elsevier Inc., 2018.

(33) Al Aani, S.; Mustafa, T. N.; Hilal, N. Ultrafiltration Membranes for Wastewater and Water Process Engineering: A Comprehensive Statistical Review over the Past Decade. *J. Water Process Eng.* **2020**, *35*, 101241.

(34) Mänttäri, M.; Nyström, M.; Nuortila-Jokinen, J.; Kallioinen, M. Nanofiltration in the Pulp and Paper Industry. *Nanofiltration* **2021**, 599–620.

(35) Geise, G. M. Why Polyamide Reverse-Osmosis Membranes Work so Well. *Science (80).* **2021**, *371* (6524), 31–32.

(36) Teixeira, M. R.; Rosa, M. J.; Nyström, M. The Role of Membrane Charge on Nanofiltration Performance. *J. Memb. Sci.* **2005**, *265* (1), 160–166..

(37) Seidel, A.; Waypa, J. J.; Elimelech, M. Role of Charge (Donnan) Exclusion in Removal of Arsenic from Water by a Negatively Charged Porous Nanofiltration Membrane. *Environ. Eng. Sci.* **2001**, *18* (2), 105–113.

(38) Van Der Bruggen, B.; Vandecasteele, C.; Van Gestel, T.; Doyen, W.; Leysen, R. A Review of Pressure-Driven Membrane Processes in Wastewater Treatment and Drinking Water Production. *Environ. Prog.* **2003**, *22* (1), 46–56.

(39) Baticle, P.; Kiefer, C.; Lakhchaf, N.; Larbot, A.; Leclerc, O.; Persin, M.; Sarrazin, J. Salt Filtration on Gamma Alumina Nanofiltration Membranes Fired at Two Different Temperatures. *J. Memb. Sci.* **1997**, *135* (1), 1–8.

(40) Ratanatamskul, C.; Urase, T.; Yamamoto, K. Description of Behavior in Rejection of Pollutants in Ultra Low Pressure Nanofiltration. *Water Sci. Technol.* **1998**, *38* (4), 453–462.

(41) Xu, X.; Spencer, H. G. Transport of Electrolytes through a Weak Acid Nanofiltration Membrane: Effects of Flux and Crossflow Velocity Interpreted Using a Fine-Porous Membrane Model. *Desalination* **1997**, *113* (1), 85–93.

(42) Mulder, M.; Mulder, J. *Basic Principles of Membrane Technology*; Kluwer Academic Publishers, 1996.

(43) Xu, Y.; Lebrun, R. E. Comparison of Nanofiltration Properties of Two Membranes Using Electrolyte and Non-Electrolyte Solutes. *Desalination* **1999**, *122* (1), 95–105.

(44) Cancino-Madariaga, B.; Hurtado, C. F.; Ruby, R. Effect of Pressure and PH in Ammonium Retention for Nanofiltration and Reverse Osmosis Membranes to Be Used in Recirculation Aquaculture Systems (RAS). *Aquac. Eng.* **2011**, *45* (3), 103–108.

(45) Paugam, L.; Taha, S.; Dorange, G.; Jaouen, P.; Quéméneur, F. Mechanism

of Nitrate Ions Transfer in Nanofiltration Depending on Pressure, PH, Concentration and Medium Composition. *J. Memb. Sci.* **2004**, *231* (1–2), 37–46.

(46) Wenten, I. G.; Khoiruddin. Reverse Osmosis Applications: Prospect and Challenges. *Desalination* **2016**, *391*, 112–125.

(47) Van der Bruggen, B.; Schaep, J.; Wilms, D.; Vandecasteele, C. Influence of Molecular Size, Polarity and Charge on the Retention of Organic Molecules by Nanofiltration. *J. Memb. Sci.* **1999**, *156* (1), 29–41.

(48) Nyström, M.; Kaipia, L.; Luque, S. Fouling and Retention of Nanofiltration Membranes. *J. Memb. Sci.* **1995**, *98* (3), 249–262.

(49) Liu, X.; Wang, W. The Application of Nanofiltration Technology in Recovery of Ionic Liquids from Spinning Wastewater. *Appl. Mech. Mater.* **2012**, *178–181*, 499–502.

(50) Al-Sofi, M. A. K.; Hassan, A. M.; Mustafa, G. M.; Dalvi, A. G. I.; Kither, M. N. M. Nanofiltration as a Means of Achieving Higher TBT of ≥ 120°C in MSF. *Desalination* **1998**, *118* (1), 123–129.

(51) Nilsson, M.; Trägårdh, G.; Östergren, K. The Influence of PH, Salt and Temperature on Nanofiltration Performance. *J. Memb. Sci.* **2008**, *312* (1–2), 97–106.

(52) Roy, Y.; Warsinger, D. M.; Lienhard, J. H. Effect of Temperature on Ion Transport in Nanofiltration Membranes: Diffusion, Convection and Electromigration. *Desalination* **2017**, *420* (August), 241–257.

## Table of Content - TOC

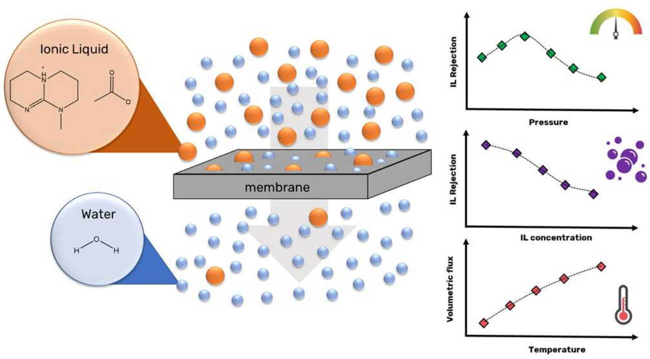


**Synopsis.** The separation of superbase ILs from water using membrane filtration is herein demonstrated to highlight the challenges in recovering hydrophilic ILs from aqueous solutions.